MAGNETOHYDRODYNAMICS Vol. 52 (2016), No. 1, pp. 15–24

MHD DYNAMO IN A DEAN-LIKE FLOW INSIDE A TORUS

A. Chupin[1,2,3]

[1] *Institute of Continuous Media Mechanics, Perm, Russia*
[2] *Perm National Research Polytechnic University, Russia*
[3] *Perm State National Research University, Russia*

Implementation of magnetohydrodynamic dynamo requires flows of a quite complicated configuration. One of the simplest dynamo models is the Ponomarenko model representing screw motion of a rigidly rotating cylinder in an infinite conducting medium. However, it is not necessary to have a special helical configuration of ducts or devices to produce helicity in a flow of an incompressible viscous fluid. A pressure-driven flow inside a curved channel, commonly known as the Dean flow, possesses its own non-zero helicity. Our simulations give evidences that such flow of conducting medium is sufficient for the self-generation of a magnetic field.

Introduction. At present, the magnetohydrodynamic (MHD) dynamo theory is widely recognized as an explanation of the existing configurations of magnetic fields in many astronomical objects, from planets like the Earth to galaxy clusters. The main mechanism of the self-generation of magnetic field is that the motion of a conducting fluid "stretches, twists and folds" [1] the frozen magnetic lines, thus multiplying the magnetic flux. Kinetic energy of the fluid is transformed into magnetic energy, and a new field is induced in the conducting medium in addition to the existing seed field. The difficulty in discovering the phenomenon was caused by the complexity of the motion which cannot be plane or axisymmetric as it is shown by the so-called anti-dynamo theorems. A large-scale dynamo has a threshold nature and, therefore, a flow of rather high intensity is required for the magnetic field generation. This imposes some restrictions on the possibility of laboratory experiments.

One of the first dynamo models that had played an important role in finding MHD models was the model of Ponomarenko [2]. Besides its simplicity (helical motion of a rigid electrically conducting cylinder of infinite length through an infinitely extended medium of the same conductivity), the Ponomarenko model delivers the lowest known threshold (7) due to an unrealistic infinite conducting medium and a discontinuous velocity profile [3]. Using the Ponomarenko model, several authors have proposed a family of screw dynamo models, involving continuous and hydrodynamically realistic velocity fields [4–6]. Some of these models have been chosen for implementation under laboratory conditions.

The magnetic field generation usually requires very powerful pumps and large amounts of liquid metal. For this reason, so far, only few successful laboratory MHD dynamo experiments have been conducted [7–9] along with some experiments in which conditional or non-purely hydrodynamical dynamo action was observed [10]. Suitable models are still in search. The flow screw configuration was created by long spiral-type pipes [7, 8] and/or by helicity-generating propelleres [9].

Another approach derived from the Ponomarenko model has been developed in the Laboratory of Physical Hydrodynamics at the Institute of Continuous Media Mechanics, Perm, Russia [11]. This approach implies that a toroidal channel filled with liquid sodium rotates around the channel axis. The flow driven by abrupt breaking of the rotation gains helicity moving along the propellers rigidly fixed inside the channel. The model has two specific features: a small amount of liquid sodium and strong non-stationarity of the process. The possibility to reach the dynamo threshold was predicted theoretically [12] and numerically [13]. The properties of the generated magnetic field caused by the discrete spectrum along the finite channel length and the influence of the flow in the opposite part of the torus on the magnetic field generation were analyzed in [14]. In [15], we demonstrated that a global mode can be generated in a thick torus.

The main message of this paper is that a helical motion does not necessarily requires a special helical configuration of ducts or helicity-generating devices. It was first shown by Dean [16] that the pressure-driven flow inside the curved channel possesses its own helicity. In this flow, the total helicity is zero, but there are two symmetrical sign-opposite helicity regions which should be enough to not violate the anti-dynamo theorems. We show that this is a sufficient condition for dynamo action.

The problem of finding velocity fields in curved channels is fully nonlinear and, therefore, it is difficult to derive exact solutions even for the simplest case of stationary pressure-driven flow inside a rigid motion-free horizontal channel of circular cross-section. Different approaches have been used to find a solution to this problem [17]. There have been several attempts to measure a velocity profile experimentally [12, 18, 19]. Most works use numerical simulations to calculate the velocity components for different parameters. A thorough review of the numerical studies on toroidal flows is presented in [20].

In the limit of small Reynolds numbers Re, the nonlinear interaction between centrifugal forces and Coriolis forces is inessential, and some simplifications can be made for the governing equations [21]. In this case, one governing parameter (the Dean number combines flow intensity and channel curvature) is sufficient to describe different flow characteristics, and the solution has two counter-rotating vortices ("Dean vortices") in the cross-section [20]. These vortices represent the velocity components $\mathbf{V}_{\text{sec}}$. At the same time, the maximum of the axial velocity U moves to the outer boundary, and the mean flow (flowrate) decreases [22]. With increasing Reynolds number, there occur bifurcations which give rise to unstable and stable flows with different patterns [23, 24] of secondary flow vortices or stream velocity profiles. Nevertheless, a transition to turbulence takes place in curved pipes at higher Reynolds numbers if compare to straight ones [25].

Analytical investigations cannot provide a solution to the problem with moderate Reynolds numbers. These studies employ a series expansion in powers of the small parameter of curvature [16, 19] and different asymptotic approaches (boundary layer, Polhausen method) for high Reynolds numbers [26]. There are arguments that theoretical models can give inexact results [27].

The kinematic dynamo approach suggests that a magnetic field is small and the velocity field remains unchanged. On the contrary, the nonlinear MHD problems consider the mutual influence of both fields. The non-linear interaction in Ponomarenko-like dynamos has been extensively investigated by the Riga group, and the research results are presented in [28]. The magnetic field can also influence hydrodynamic stability [29].

We have failed to find studies investigating the possibility of magnetic field self-generation by non-constrained flows in a duct of such a simple form. The purpose of our study is to fill this gap and to consider the opportunity to implement our MHD dynamo model under laboratory conditions.

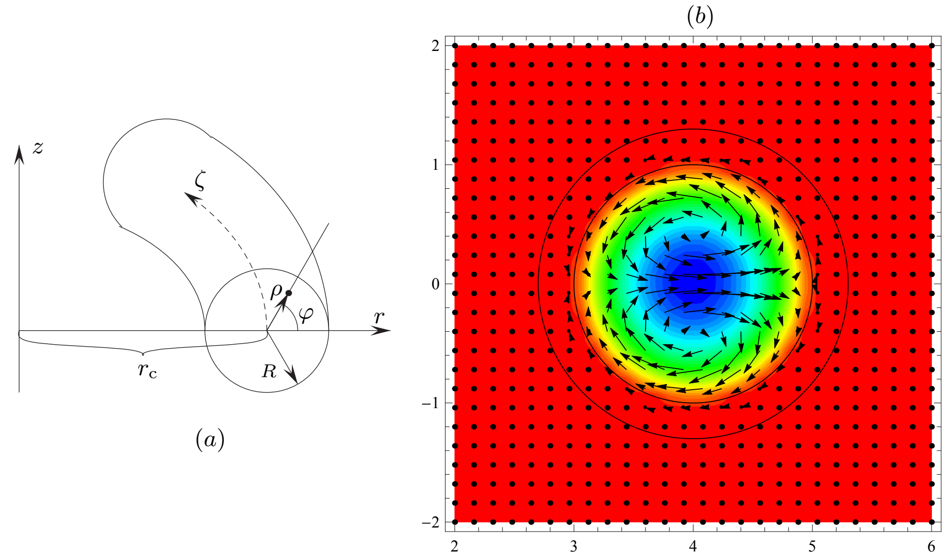

Fig. 1. Coordinates (a) and velocity field (b) used in a Dean-like dynamo model.

1. Governing equations. Consider a toroidal channel filled with an electrically conducting fluid. In order to compare our model with the classical Ponomarenko model, the electrical conductivities of the channel walls and external medium (the ordinary air in laboratory experiments) are assumed to be equal to the conductivity of the fluid η. The torus is characterized by the outer radius R_o and the radius of its cross-section R_i.

We use the cylindrical coordinates r, ζ, z which are shown in Fig. 1a. The polar coordinates ρ, ϕ in the cross-section correspond to the model described in [30] and are used to define the velocity field.

The following values of the physical quantities are taken as characteristic units: the inner radius R_i of the channel as the characteristic length, the stream velocity U as the characteristic velocity, and the diffusion time R_i^2/η as the characteristic time. Hence, we have $\kappa = R_\mathrm{i}/R_\mathrm{o}$ as a single geometrical parameter, the magnetic Reynolds number $\mathrm{Rm} = UR_\mathrm{i}/\eta$ as a measure of flow intensity with respect to diffusion, and the ratio of cross-section velocity to stream velocity $\chi = V_\mathrm{sec}/U$ as a flow pitch.

In the case of moving conducting medium, the dimensionless evolution equations for the magnetic induction $\mathbf{B}$ can be written as (1)

$$\partial \mathbf{B}/\partial t = \mathrm{Rm}\,\mathrm{rot}\,(\mathbf{v} \times \mathbf{B}) - \mathrm{rot}\,(\mathrm{rot}\,\mathbf{B})\,, \tag{1}$$

$$\mathrm{div}\mathbf{B} = 0. \tag{2}$$

To tackle the difficulty with the magnetic induction solenoidality (2), instead of Eq. (1), we use the equations for the magnetic vector potential $\mathbf{A}$ defined as

$$\mathbf{B} = \mathrm{rot}\,\mathbf{A}. \tag{3}$$

The vector potential is insensitive to an arbitrary additive potential field. Substituting Eq. (3) into Eq. (1) yields

$$\partial \mathbf{A}/\partial t = \mathrm{Rm}\,(\mathbf{v} \times \mathbf{A}) + \triangle \mathbf{A} - \mathrm{grad}\,\mathrm{div}\mathbf{A} + \mathrm{grad}\,\Phi, \tag{4}$$

where Φ is the electric potential, which in our study is taken equal to div$\mathbf{A}$ to cancel the last two terms. Introducing the vector potential also allows us to use non-continuous velocity profiles without additional care. It is difficult to specify boundary conditions for the magnetic field because it extends to infinity. To perform simulations within the finite region, we use an assumption that the electric current does not pass beyond the region. In terms of the vector potential, this condition can be expressed as $A_\perp = 0$, $\partial A_\parallel/\partial \mathbf{n} = 0$ ($\mathbf{n}$ here stands for the normal direction).

In our investigation, we seek a solution to the instability problem of a trivial magnetic field and, therefore, we can use a small uniformly distributed random field as the initial field because it contains all harmonics. For faster convergence, we also use a pre-calculated dynamo wave obtained from runs with similar parameters.

Simulations were performed for laminar flow in the form of two symmetrical Dean vortices. This flow corresponds to the first order approximation obtained in [30]. Although the actual flow inside a torus is often created by rotation and the Coriolis force can influence the flow pattern [17], we do not consider the rotation effects in this paper (using the notation of [17], $F = 0$).

So we define the dimensionless velocity (Fig. 1*b*) as

$$\mathbf{v} = (1-\rho^2)\left[\frac{\chi\mathrm{Re}}{288}\Big(\cos\phi\left(1-\rho^2\right)\left(4-\rho^2\right)\mathbf{e}_\rho + \sin\phi\left(10-53\rho^2+7\rho^4\right)\mathbf{e}_\phi\Big) + \mathbf{e}_\zeta\right]. \quad (5)$$

Now one can compare this velocity with the velocity field used in the Ponomarenko-like dynamo model [15]:

$$\mathbf{v} = \frac{\rho\chi}{(1-\kappa\rho\cos\phi)\sqrt{1+\chi^2}}\,\mathbf{e}_\phi + \frac{1}{\sqrt{1+\chi^2}}\,\mathbf{e}_\zeta. \quad (6)$$

As shown in [30], the pitch ratio χ strongly influences the thresholds. In real flows inside the torus, the cross-section velocity components are much less than the stream component, but they exhibit a non-monotonic character (Fig. 2). The maximum pitch ratio is estimated as $\sim 1/3$.

2. Kinematic dynamo. The dynamo wave is the eigenfunction of the main equations, it can be identified by the complex increment $\gamma + i\omega$ in time and wave number k along the channel. The wave number varies inversely as the wave length, so for the finite length of the toroidal channel there is a discrete spectrum of wave numbers. As related to the inner radius, we have the following restriction to the dimensionless wave number: $k_n = n\kappa = (nR_\mathrm{i})/R_\mathrm{o}$.

The condition $\gamma = 0$ corresponds to a threshold situation when the magnetic field has a stationary magnitude, and the imaginary part of the increment is a time frequency of the magnetic field oscillations. The corresponding critical magnetic Reynolds number depends on the wave number k as well as on the flow parameter χ (Fig. 3).

The global minimum threshold for the self-generation of the magnetic field by the solid-like motion of a conducting cylinder in the conducting environment is $\mathrm{Rm}_\mathrm{cr} = 17.7$ at $\chi = 1$ and has $k = 0.67$.

$$\mathrm{Rm} = UR_\mathrm{i}\,\eta^{-1} = 17.7. \quad (7)$$

The discrete nature of the wave numbers in the torus leads to a situation when for each κ a minimum threshold can be reached at different χ, as shown in Fig. 3 of [30]. For example, $\mathrm{Rm}_\mathrm{cr}\,(\kappa = 2.5, \chi = 1) = 25$ and $\mathrm{Rm}_\mathrm{cr}\,(\kappa = 2.5, \chi = 1.3) = 19$.

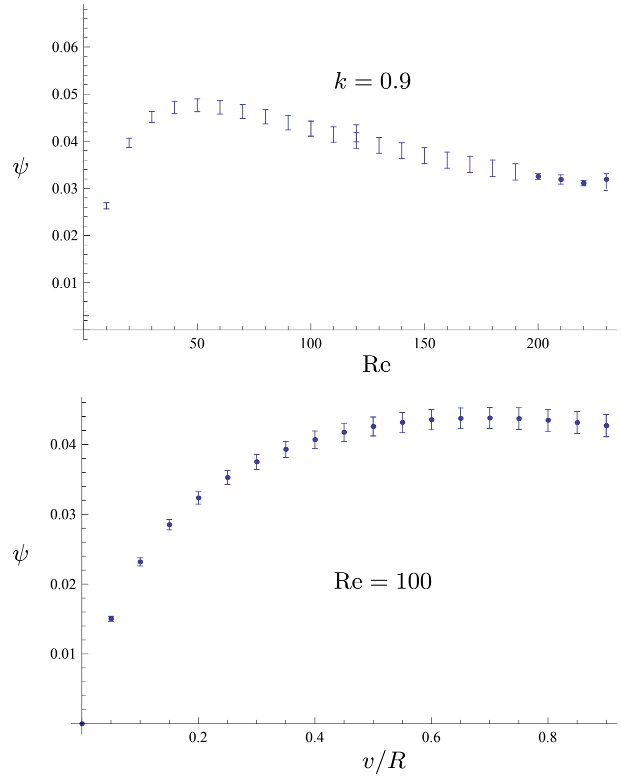

Fig. 2. Maximum of the cross-section stream function vs. the Reynolds number at $\kappa = 0.9$ and vs. the torus curvature κ at $\mathrm{Re} = 100$.

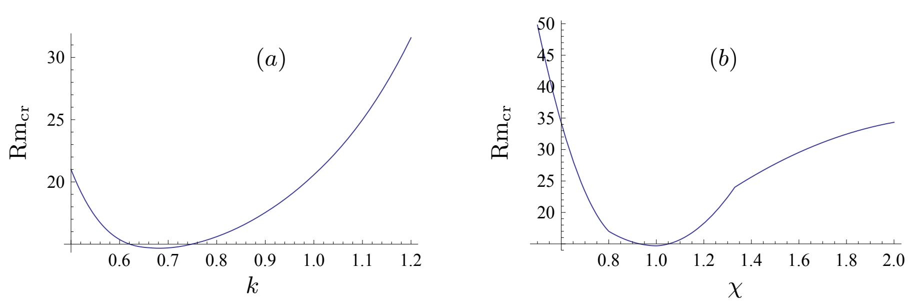

Fig. 3. Critical magnetic Reynolds numbers in Ponomarenko dynamo: (*a*) $\mathrm{Rm_{cr}}(k)$, (*b*) $\mathrm{Rm_{cr}}(\chi)$.

3. Numerical methods. The numerical method is in general the same as in [15, 30]. Briefly, direct numerical simulations of Eq. (4) are performed using the finite difference method. We applied the Runge–Kutta–Fehlberg scheme to advance in time and to determine the increment $\gamma + i\omega$ of the dynamo wave from a time series. For fast search of the thresholds, an adaptive change of the magnetic Reynolds number during some runs was employed.

Because of the pervasive magnetic field, a simulation was conducted on a rectangular grid in a cuboid (in the coordinates r, ζ, z) region which extends to a distance of R_i from the border of the channel. The program has been upgraded for parallel computing. To this end, the whole simulation region is decomposed into subregions, each assigned to a different processor. All simulations were done

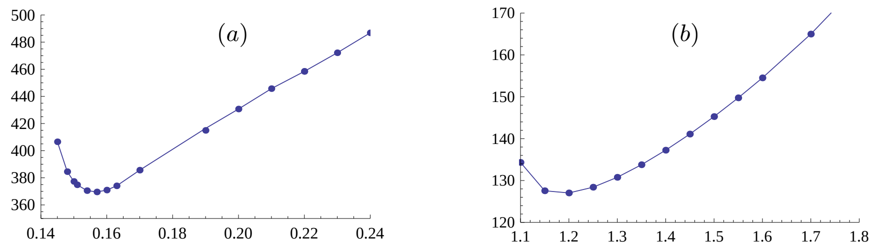

Fig. 4. Thresholds in a Dean-like flow vs. the wave number: (a) at $\chi = 0.3$; (b) at $\chi = 1.6$.

using the supercomputers of the Ural Branch of the Russian Academy of Sciences (Triton at ICMM and URAN at IMM).

Tests have shown that the increments in the simulations with the mesh resolution $32 \times 32 \times 32$ do not deviate from the increments with the resolution 256^3 by more than 1%, and thus the main plots were obtained for the mesh resolution $32 \times 32 \times 32$. A typical run to find one threshold lasted 2 to 10 hours with 32–64 processors.

Simulations were performed for some part of the torus of the length l (as shown in Fig. 1a). In such region, the generated dynamo waves have wave numbers $k \vdots (2\pi)/l$. For the chosen set of the parameters $\kappa, \chi, \mathrm{Rm}$ and fixed velocity field (5), we marched in time according to Eqs. (4) until the magnetic field demonstrated a purely exponential growth. Then we adjusted Rm in order to find a neutral growth (when $\gamma = 0$). Thus we obtained the thresholds as a function of the governing parameters, i.e. $\mathrm{Rm}_{\mathrm{cr}}(\kappa, \chi, k)$.

4. Results. We restricted our study to a case of a toroidal channel of moderate thickness. The effects of the flow in the opposite part of the torus were ignored, but the channel curvature and finiteness were taken into account. We used $\kappa = 0.25$.

For each velocity field, we sought an optimal wave number, as shown in Fig. 4. Theoretically, the optimal geometry of the flow should have $\chi \approx 1.6$ (see Fig. 5).

For such velocity field, the critical magnetic Reynolds number is as low as $\mathrm{Rm}_{\mathrm{cr}} = 126.77$ having a wave number $k \approx 1.18$.

Generally, the wave number of optimal dynamo waves depends nearly proportionally on χ (Fig. 6a). A similar picture is observed for Ponomarenko-like dynamo in a torus.

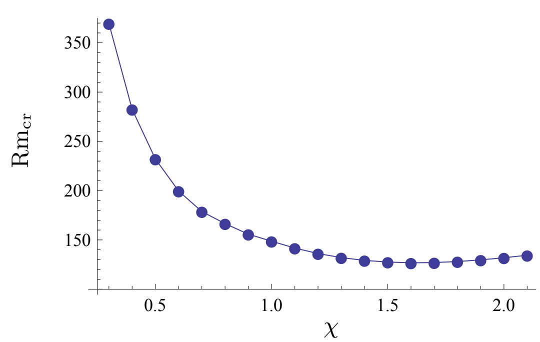

Fig. 5. Thresholds in a Dean-like flow vs. χ.

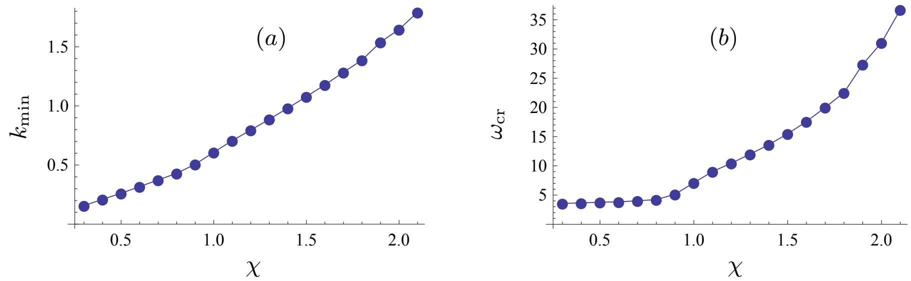

Fig. 6. Characteristics of optimal dynamo waves vs. χ: (*a*) wave numbers for critical Reynolds numbers; (*b*) rotation rates of optimal dynamo waves.

Interestingly, the rotation rate of such waves also decreases as the intensity of the secondary component of the flow reduces (Fig. 6*b*). On the contrary, in Ponomarenko-like dynamo, the rotation rate depends mainly on the absolute value of the threshold and hence the rotation rate decreases when χ increases from 0.3 to 1.6.

Magnetic field distributions are presented in Figs. 7–8, where the magnetic field components are shown for three cross-sections of the channel. The arc-shaped sections, involving ζ as one of the coordinates, are straightened to a rectangular shape. The hue shows the magnitude of the field component perpendicular to the cross-section, and the vectors shows the field components in the cross-section.

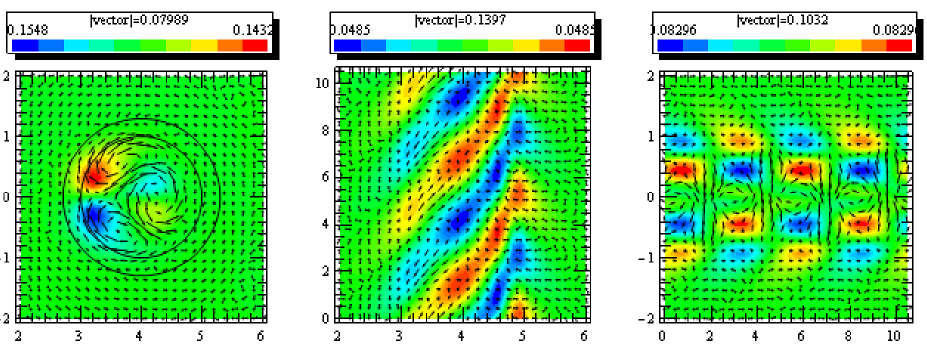

Fig. 7. Neutral dynamo wave with the global minimum threshold $\kappa = 0.25$, $\chi = 1.5$, $k = 0.55$, $\mathrm{Rm} \approx 128$.

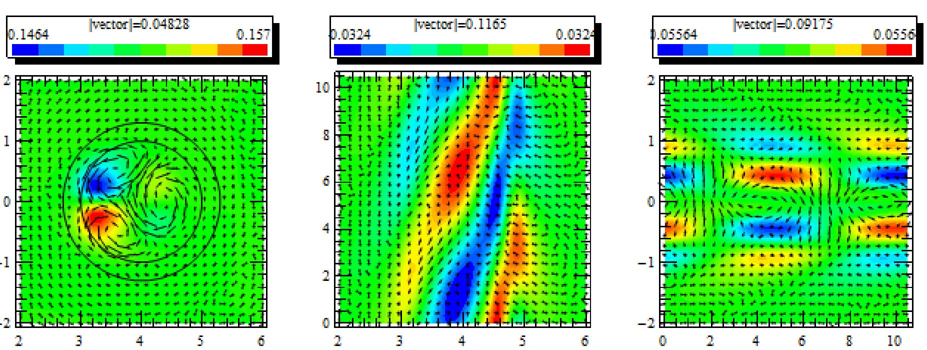

Fig. 8. Neutral dynamo wave for possible geometry of the flow $\kappa = 0.25$, $\chi = 1$, $k = 0.75$, $\mathrm{Rm} \approx 159$.

The magnetic field has a structure of two dynamo waves interwoven in the symmetry plane and its magnitude outside the channel decreases rapidly. The distribution of each wave in the cross-section has only one pronounced maximum, as opposed to "yin and yang" picture of maxima in Ponomarenko-like dynamos.

In order to compare our results with the classical minimum (7), we have also calculated the thresholds for Ponomarenko-like dynamo in a torus for parameters similar to those used in the present study. We considered the parabolic profile of the stream velocity and the cross-section components from Eq. (6). For $\chi = 0.3$, we had a neutral dynamo wave with $\mathrm{Rm} \approx 62.3$, the wave number $k \approx 0.23$ and the rotation frequency $\omega \approx 2.35$. For $\chi = 1.6$, the threshold reduced to $\mathrm{Rm} \approx 22.6$, the rotation frequency decreased to $\omega \approx 1.8$ and the wave number increased to $k \approx 1.07$.

5. Conclusions. Our simulations have confirmed that in many aspects the dynamo action in Dean-like flows is similar to that in the Ponomarenko model. Similarly, a dynamo wave whose characteristics depend on the flow pitch can be generated. It is shown that its critical magnetic Reynolds number is dependent on its wave number, and the wave number of the optimal dynamo wave behaves similarly, as the pitch of the flow changes.

The differences between the models are the following. Due to the existence of two vortices in the cross-section, Dean-like dynamo has two interwoven dynamo waves instead of one, as in the Ponomarenko case. The distribution of the magnetic field in the cross-section is somewhat different as well. The rotation rates of the waves are defined by the pitch of the flow rather than by the magnetic Reynolds number.

Summing up, Dean-like flows can maintain the dynamo action. However, it should be noted that the magnetic Reynolds threshold obtained in our study is roughly six times higher than that described by the Ponomarenko model and, therefore, can hardly be reached experimentally. On the other hand, the absence of breakers inside the channel makes the construction more robust, facilitating the generation of the necessary intensity of the flow.

We have set a fixed velocity field, whereas in reality its shape depends on the torus curvature and on the hydrodynamic Reynolds number. Further research is needed to derive dynamo characteristics in real configurations of laminar and turbulent flows. Also the regimes should be investigated in which the magnetic field affects the flow.

Acknowledgements. All computations were made with the use of the supercomputer Triton at the Institute of Continuum Media Mechanics (Perm, Russia).

The author would like to thank the Laboratory of Physical Hydrodynamics of ICMM UB RAS and especially R. Stepanov and P. Frick for useful discussions during the analysis of the results.

References

[1] S. Childress and A.D. Gilbert. *Stretch, Twist, Fold* (Springer Science & Business Media, 1995).

[2] Y.B. Ponomarenko. On the theory of the hydromagnetic dynamo. *JAMTP*, vol. 14 (1973), no. 6, pp. 775–778.

[3] A. Gailitis and Ya. Freiberg. Contribution to helical MHD dynamo theory. *Magnetohydrodynamics*, vol. 12 (1976), no. 2, pp. 127–129

[4] A. Ruzmaikin, D. Sokoloff, and A. Shukurov. Hydromagnetic screw dynamo. *Journal of Fluid Mechanics*, vol. 197 (1988), pp. 39–56.

[5] E. A. Lupian and A. Shukurov. The screw dynamo in real flows. *Magnetohydrodynamics*, vol. 28 (1992), no. 3, pp. 234–240,

[6] A. Basu. Screw dynamo and the generation of nonaxisymmetric magnetic fields. *Phys. Rev. E*, vol. 56 (1997), pp. 2869–2874.

[7] A. Gailitis, *et al.* Detection of a flow induced magnetic field eigenmode in the riga dynamo facility. *Phys. Rev. Lett.*, vol. 84 (2000), pp. 4365–4368.

[8] U. Müller and R. Stieglitz. The karlsruhe dynamo experiment. *Nonlinear Processes in Geophysics*, vol. 9 (2002), pp. 165–170.

[9] R. Monchaux, *et al.* Generation of a magnetic field by dynamo action in a turbulent flow of liquid sodium. *Phys. Rev. Lett.*, vol. 98 (2007), p. 044502.

[10] A. Tilgner. Laboratory dynamo experiments and what we learned from them. *Astronomische Nachrichten*, vol. 323 (2002), pp. 407–410.

[11] S.A. Denisov, *et al.* On the possibility of laboratory realization of an unsteady mhd-dynamo. *Physics-Doklady*, vol. 44 (1999), pp. 231–233.

[12] P. Frick, *et al.* Non-stationary screw flow in a toroidal channel: way to a laboratory dynamo experiment. *Magnetohydrodynamics*, vol. 38 (2002), no. 1–2, pp. 143–162.

[13] W. Dobler, A. Shukurov, and A. Brandenburg. Nonlinear states of the screw dynamo. *Physical Review E*, vol. 65 (2002), no. 3, p. 36311.

[14] R. Stepanov, A. Chupin, and P. Frick. Screw dynamo in a torus. *Comp. Continuum Mech.*, vol. 1 (2008), pp. 109–117.

[15] A. Chupin, P. Frick, and R. Stepanov. The screw dynamo in a thick torus. *Astronomische Nachrichten*, vol. 332 (2011), no. 1, pp. 11–16.

[16] W.R. Dean. Note on the motion of fluid in a curved pipe. *Philos. Mag.*, vol. 7 (1927), p. 208.

[17] H. Ito. Flow in curved pipes. *JSME international journal : bulletin of the JSME*, vol. 30 (1987), no. 262 (19870400), pp. 543–552.

[18] C.M. White. Streamline flow through curved pipes. *Royal Society of London Proceedings Series A*, vol. 123 (1929), pp. 645–663.

[19] M. Adler. Strömung in gekrümmten rohren. *ZAMM - Journal of Applied Mathematics and Mechanics / Zeitschrift für Angewandte Mathematik und Mechanik*, vol. 14 (1934), no. 5, pp. 257–275.

[20] W.M. Collins and S.C.R. Dennis. The steady motion of a viscous fluid in a curved tube. *The Quarterly Journal of Mechanics and Applied Mathematics*, vol. 2 (1975), no. 28, pp. 133–156.

[21] D.J. McConalogue and R.S. Srivastava. Motion of a fluid in a curved tube. *Royal Society of London Proceedings Series A*, vol. 307 (1968), pp. 37–53.

[22] D. Greenspan. Secondary flow in a curved tube. *Journal of Fluid Mechanics*, vol. 57 (1973), pp. 167–176.

[23] S.C.R. Dennis and M. Ng. Dual solutions for steady laminar flow through a curved tube. *Q. B. Mech. appl. Math.*, vol. XXXV (1981), no. 3, pp. 305–324.

[24] P. Daskopoulos and A.M. Lenhoff. Flow in curved ducts - bifurcation structure for stationary ducts. *Journal of Fluid Mechanics*, vol. 203 (1989), pp. 125–148.

[25] G.I. Taylor. The criterion for turbulence in curved pipes. *Royal Society of London Proceedings Series A*, vol. 124 (1929), pp. 243–249.

[26] S.C.R. Dennis and N. Riley. On the fully developed flow in a curved pipe at large dean number. *Royal Society of London Proceedings Series A*, vol. 434 (1991), pp. 473–478.

[27] S. Jayanti and G.F. Hewitt. On the paradox concerning friction factor ratio in laminar flow in coils. *Royal Society of London Proceedings Series A*, vol. 432 (1991), pp. 291–299.

[28] A. Gailitis, *et al.* History and results of the riga dynamo experiments. *Comptes Rendus Physique*, vol. 9 (2008), no. 7, pp. 721–728.

[29] M. Hoque, N.N. Anika, and M. Alam. Numerical analysis of magnetohydrodynamics flow in a curved duct. *International Journal of Scientific & Engineering Research*, vol. 4 (2013), no. 7, pp. 607–617.

[30] A. Chupin and R. Stepanov. Full perturbation solution for the flow in a rotating torus. *Physical Review E*, vol. 77 (2008), no. 5, p. 057301.

Received 30.11.2015